

# Evaluation of pedotransfer functions for estimating saturated hydraulic conductivity in coastal salt-affected mud farmland

Rong-Jiang Yao · Jing-Song Yang · Dan-Hua Wu ·  
Fu-Rong Li · Peng Gao · Xiang-Ping Wang

Received: 17 August 2014 / Accepted: 22 December 2014 / Published online: 8 January 2015  
© Springer-Verlag Berlin Heidelberg 2015

## Abstract

**Purpose** Pedotransfer functions (PTFs) have gained wide development in recent years as approaches to establishing the relationship between easily measurable or readily available soil characteristics found in soil surveys and more complicated model input parameters. However, PTFs developed from databases with limited types of soil conditions might not be directly applicable to other soils whose conditions are different from those used to establish PTFs. Our primary objectives were to determine the influencing factors of saturated hydraulic conductivity ( $K_s$ ) in the coastal salt-affected farming area, to identify the most appropriate one from the widely used PTFs, and to develop new PTFs with higher accuracy and suitability according to the influencing factors of  $K_s$  in our experimental sites.

**Materials and methods** A total of 16 soil attributes including 9 physical properties and 7 chemical properties, which were collected in typical coastal newly reclaimed farmlands of north Jiangsu Province, China, were used as input soil data of the PTFs. Factor analysis was employed to group soil basic properties into influencing factors of  $K_s$ . The appropriate PTFs were identified according to the prediction criteria, and new PTFs were established using multiple linear regression,

modified Vereecken PTF, and artificial neural network methods.

**Results and discussion** Results indicated that  $K_s$  in the soil profile was classified as low permeability and 20–40-cm layer (Ap2 horizon) had the lowest  $K_s$  and highest bulk density values. With 91.05 % of variance explained, the 16 soil basic properties were classified into five factors, i.e., soil porosity component, water retention component, organic matter component, soil salinity component, and unavailable water component. Among all the selected PTFs, Ahuja PTF was identified as the most convenient method which only needed effective porosity. Vereecken PTF was suitable for a wider range of soil textural classes. Using  $S_A$ ,  $C_L$ ,  $B_d$ , SOM, and  $EC_e$  as input soil data, the modified Vereecken (MV) PTF and artificial neural network (ANN) PTF had better prediction performance than the published PTFs.

**Conclusions** We concluded that soil salinity played an important role in the estimation of  $K_s$  and should be considered as input soil data. The established ANN-based PTF using the suggested input soil data was recommended as the best approach for estimation of soil  $K_s$  in the coastal salt-affected farming area.

**Keywords** Coastal · Influencing factor · Pedotransfer function · Reclaimed farmland · Saturated hydraulic conductivity

Responsible editor: Ying Ouyang

R.-J. Yao · J.-S. Yang · F.-R. Li · X.-P. Wang  
State Key Laboratory of Soil and Sustainable Agriculture, Institute of  
Soil Science, Chinese Academy of Sciences (CAS), Nanjing 210008,  
China

R.-J. Yao · J.-S. Yang (✉) · D.-H. Wu  
Dongtai Institute of Tidal Flat Research, Nanjing Branch of the  
Chinese Academy of Sciences, Dongtai 224200, China  
e-mail: jsyang@issas.ac.cn

P. Gao  
Department of Geography, University of South Carolina, 709 Bull  
Street, Columbia, SC 29208, USA

## Abbreviations

$S_A$	Content of sand particles (%)
$S_I$	Content of silt particles (%)
$C_L$	Content of clay particles (%)
$B_d$	Bulk density ( $\text{g cm}^{-3}$ )
$T_{Por}$	Total porosity
$E_{Por}$	Effective porosity
$\theta_s$	Soil saturated water content ( $\text{cm}^3 \text{cm}^{-3}$ )
$\theta_{fc}$	Field capacity ( $\text{cm}^3 \text{cm}^{-3}$ )

$\theta_w$	Wilting point ( $\text{cm}^3 \text{cm}^{-3}$ )
$EC_e$	Electrical conductivity of saturated soil paste extract ( $\text{dS m}^{-1}$ )
$SAR$	Sodium adsorption ratio
$SOM$	Soil organic matter ( $\text{g kg}^{-1}$ )
$TN$	Soil total nitrogen ( $\text{g kg}^{-1}$ )
$AN$	Available nitrogen ( $\text{mg kg}^{-1}$ )
$AP$	Available phosphate ( $\text{mg kg}^{-1}$ )
$AK$	Available potassium ( $\text{mg kg}^{-1}$ )
$K_s$	Saturated soil hydraulic conductivity ( $\text{cm day}^{-1}$ )
$PTFs$	Pedotransfer functions

## 1 Introduction

Reliable information about soil hydraulic properties plays an important role in solving many soil and water management problems related to agriculture, ecology, and environmental issues. These properties are indispensable to describe and predict water and solute transport, as well as to model heat and mass transport near the soil surface (Cornelis et al. 2001). One of the key soil hydraulic properties is the saturated hydraulic conductivity ( $K_s$ ) which is an important soil physical property for assessing infiltration rate, irrigation practice and drainage design and in modeling the agricultural and hydrological processes (Aimrun et al. 2004). This is particularly the case for the coastal farming area where high soil salinity due to very saline shallow water table is one of the most significant limitations to soil water use efficiency (Yao et al. 2012).

Using representative soil samples from the study area, soil hydraulic properties are usually measured in widely used measurement techniques, such as the Guelph permeameter in situ method (Reynolds and Elrick 1986) and the constant head permeameter laboratory method (Klute and Dirksen 1986). Other frequently used in situ method included instantaneous profile method, Wind's evaporation method, Crust method, sorptivity methods, and one-step outflow method (Xu and Liu 2003). However,  $K_s$  has high spatial variability, and large numbers of soil samples are required to characterize the hydraulic properties in the area of interest. For broad-scale applications, such measurements are often too cumbersome, expensive, time-consuming, and labor intensive. In addition,  $K_s$  exhibited scale dependency, resulting in different measurements of  $K_s$  with different size of soil samples at the same location (Sobieraj et al. 2004; Fuentes and Flury 2005). Larger size of soil samples was suggested to get reliable measurement for soils with high spatial variability of  $K_s$  (Lai and Ren 2007). Therefore, more attention has been attracted to the indirect estimation of  $K_s$ , and the interest in using pedotransfer functions (PTFs) to estimate the hydraulic property of the soil is increasing (Wagner et al. 2004; Stumpp et al. 2009; Arrington et al. 2013).

The PTFs as initially defined by Bouma and Lanen (1987) describes functions that link more easily measurable and more readily available soil properties such as particle size distribution, organic matter or organic carbon content, bulk density, and porosity to soil hydraulic characteristics. In the last three decades, a considerable number of PTFs differing in data requirements and modeling principles have been proposed in the literature, and recent reviews of the state of the art in this field of research have been given by Wösten et al. (2001), Pachepsky and Rawls (2004), and Shein and Arkhangel'skaya (2006). PTFs can be obtained by various mathematical methods. Most PTFs were derived through multiple regression methods, and Konezy-Carman equation was also applied in the PTFs (Franzmeier 1991), but the artificial neural network (ANN) approach is getting more and more popular in the recent decade. Statistical or functional comparison between the ANN-based PTFs and regression-type PTFs has been reported in detail in many literatures (Parasuraman et al. 2006; Agyare et al. 2007; Motaghian and Mohammadi 2011). Also, many sophisticated programs were developed as a convenient way for  $K_s$  prediction as yet. Schaap et al. (2001) proposed a computer program, *Rosetta*, which implemented the estimation of water retention and the saturated and unsaturated hydraulic conductivity. van Genuchten et al. (1991) established RETC computer program to analyze the soil water retention and hydraulic conductivity functions of unsaturated soils. Acutis and Donatelli (2003) developed SOILPAR software to estimate and create maps of soil hydrological parameters and functions. In addition to the traditionally used soil basic properties, investigators have attempted to incorporate new descriptors into PTFs recently, such as soil morphology (Lin et al. 1999), multistep outflow data (Minasny et al. 2004), maximum soil infiltration rates (Arrington et al. 2013), microscopic pore geometry (Lebron et al. 1999), or terrain attributes (Romano and Palladino 2002).

Coastal farming areas as reclaimed from mudflats in north Jiangsu Province, eastern China, were selected in this study. The experimental sites characterized by low soil productivity due to high soil salinity were typical of coastal newly reclaimed salt-affected soils in China. The traditional crop rotation and management systems (rice/rape rotation, cotton/barley rotation, and maize/barley rotation), representing the major crop rotation patterns in north Jiangsu Province, have been practiced in the experimental sites. To determine the appropriate PTF for the estimation of soil saturated hydraulic conductivity ( $K_s$ ), a pool of 16 basic soil properties including 9 soil physical properties and 7 soil chemical properties were selected as input soil data. Recognizing the importance of  $K_s$  in modeling soil water flow and salt transport in our experimental sites, the presented research was conducted with the following objectives: (i) to characterize the profile distribution and determine the influencing factors of  $K_s$  in the coastal salt-affected farming area, (ii) to evaluate the calibration and

prediction performance of the published PTFs and identify the most appropriate PTFs in our experimental sites, and (iii) to develop the local PTFs with higher accuracy and suitability according to the influencing factors of  $K_s$  in our experimental sites.

## 2 Materials and methods

### 2.1 Experimental site description

The experiment was carried out in the coastal salt-affected farming area in north Jiangsu Province, China. Two typical farms in this area reclaimed from mudflats were selected as the experimental sites in our study. The two farms were Jinhai Farm and Huanghai Raw Seed Growing Farm, and the two farms spaced nearly 40 km apart. Jinhai Farm was situated in the southeast of Dafeng City ( $32^{\circ} 59' \sim 33^{\circ} 01' \text{ N}$ ,  $120^{\circ} 49' \sim 120^{\circ} 51' \text{ E}$ ) and Huanghai Raw Seed Growing Farm located in the southeast of Dongtai City, which was adjacent to Dafeng City ( $32^{\circ} 38' \sim 32^{\circ} 40' \text{ N}$ ,  $120^{\circ} 52' \sim 120^{\circ} 54' \text{ E}$ ). The two farms were approximately 5 km to the coastline of China Yellow Sea, and the topography was flat with an average elevation of 1.0–1.5 m (Fig. 1).

Formed from the Yangtze River alluvial sediments and marine sediments, the predominant soil in our experimental sites is silty loam, classified as a loamy, mixed, hyperthermic, Aquic Halaquepts according to soil taxonomy (Soil Survey Staff 2010). Intermediate between an oceanic and continental climate, the experimental sites are in subtropical zone and strongly influenced by the southeast monsoon from spring to autumn and northwest monsoon in winter. Mean annual temperature is  $14.7^{\circ}\text{C}$ , mean annual evaporation is 1417 mm, and mean annual precipitation is 1042 mm (from 2001 to 2011) with approximately 67 % of annual rainfall occurring June through September. Cold, dry season is from October to March, and the hot, wet season is from April to September.

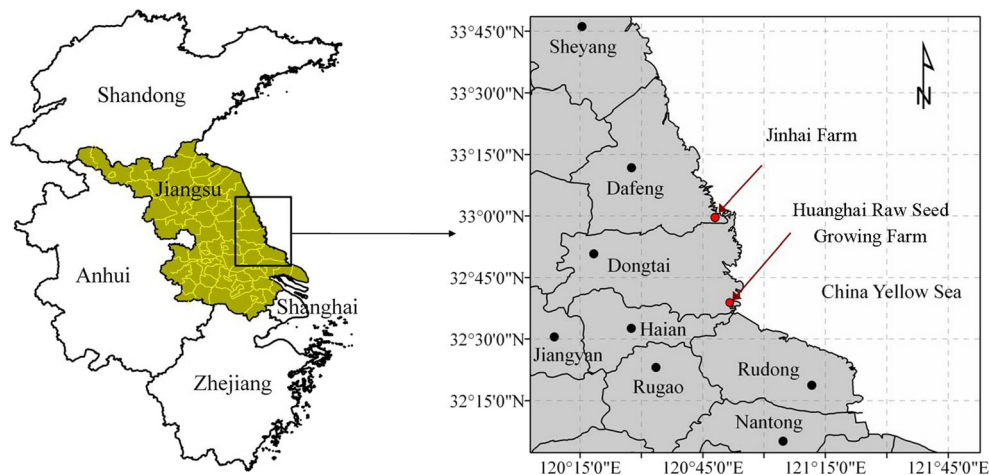
Poor soil physicochemical properties such as salinization, low fertility, and soil compaction are known as the most significant limitations to soil productivity in these farms, and large areas of salt-affected lands were observed due to high surface soil salinity as well as very saline shallow water table (Yao et al. 2009). The experimental sites cover a variety of soil salinity conditions, and they are representatives of about  $40 \times 10^4 \text{ hm}^2$  coastal salt-affected reclamation farmlands in north Jiangsu Province, Eastern China.

### 2.2 Land use and management history

The Jinhai Farm consisting of 26 stripping fields was reclaimed from mudflats in 1999 and had no documented history of cultivation until 2001. Two crop rotation systems including rice (*Oryza sativa* L.)/rape (*Brassica campestris* L.) rotation and cotton (*Gossypium* spp.)/barley (*Hordeum vulgare* L.) rotation have been practiced in this farm. The eastern portion of the farm has been in a rice/rape rotation (rice and rape in summer and winter, respectively) since its reclamation. The western portion of the farm has been consecutively cultivated with a cotton/barley rotation (cotton in summer and barley in winter) since 2005. This farm is characterized by rain-fed in barley, cotton, and rape seasons. Considering that the river water and the shallow groundwater are naturally saline in the coastal region, rice is irrigated with the freshwater which is pumped from underground wells of approximately 300–350-m depth with an electrical conductivity (EC) of 0.35 dS/m.

Huanghai Raw Seed Growing Farm was reclaimed from mudflats in 2004 and cultivated for agriculture production since 2006. A rice/barley rotation system was initially used to leach soil salinity from 2006 to 2009 as the soil reclaimed from the tidal flats contained excessive soluble salts. Likewise, the irrigation water used for paddy rice was pumped from underground wells of about 350–400-m depth with an EC of 0.47 dS/m. Due to the excessive exploitation of fresh

**Fig. 1** Geographical location of the experimental sites



groundwater and the continuous decline of the well water table, the amount of freshwater from these wells can no longer meet the water requirement of the whole farm in the paddy rice season. Thus, a rain-fed maize (*Zea mays* L.)/barley rotation system has been applied in some fields of the farm, and paddy rice has been irrigated with the mixed water of fresh deep-well water and saline river water since 2009. This phenomenon of blending irrigation is typical for extensive coastal reclamation farming areas in north Jiangsu Province.

In the experimental sites, conventional soil fertility and pest management practices are used, and paddy rice is irrigated using flood irrigation. No organic matter inputs are made other than crop residues. With diammonium phosphate as basal fertilizer, an annual of 480 kg/ha N, 210 kg/ha P<sub>2</sub>O<sub>5</sub>, and 90 kg/ha K<sub>2</sub>O is input to soil in the rice/rape rotation and rice/barley rotation systems, whereas the fertilizer of 450 kg/ha N, 180 kg/ha P<sub>2</sub>O<sub>5</sub>, and 120 kg/ha K<sub>2</sub>O is added to the cotton/barley rotation and maize/barley rotation soil. Despite the uniform management practices for each rotation system in these two farms, the crop growth varies greatly, and some spots are abandoned due to the strong spatial variation of soil conditions.

### 2.3 Soil sampling

The location and magnitude of soil samples across the experimental sites were determined considering soil salinity, vegetation canopy, and crop rotation system. A total of 124 surface soil samples at 0–10-cm depth were collected using a hand auger. Among these soil samples, 60 sites were collected from Jinhai Farm in late-October 2009, and the other 64 sites were collected from Huanghai Raw Seed Growing Farm in early-October 2012. At each site, three bulk and nine core soil samples were obtained at 0–10 cm for lab analysis of K<sub>s</sub> and other soil basic properties, and the nine replicate undisturbed core soil samples were collected using cutting rings (volume of 100 cm<sup>3</sup>) with each spaced 5 cm apart. Apart from this, in order to determine soil profile characterization, six locations were selected from Huanghai Raw Seed Growing Farm for profile excavation. At each location, soil pit from surface to 1-m depth was dug using a shovel, and horizonation was determined and recorded by a pedologist using standard methods (Schoeneberger et al. 2002). The time of soil sampling and profile excavation was just between the harvest time of rice/cotton/maize and the sowing time of rape/barley. Figure 2 visually exhibits the information and horizonation of the six representative soil profiles.

At each profile, three bulk and nine core soil samples were collected at 0–20, 20–40, 40–60, 60–80, and 80–100 cm for lab analysis of K<sub>s</sub> and other soil basic characteristics. In total, 444 bulk and 1332 core samples were collected across the experimental sites. All bulk soil samples were air-dried and passed through a 2-mm sieve prior to performing analyses of

chemical and physical properties, and core soil samples were mainly used for lab analysis of K<sub>s</sub> and some soil physical attributes.

### 2.4 Soil analysis

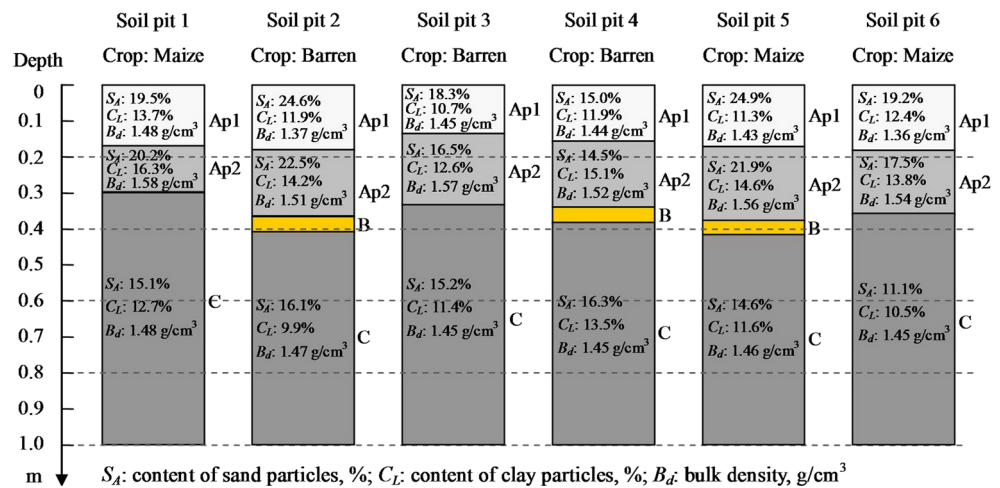
Understanding the relationship between soil basic properties and saturated hydraulic conductivity (K<sub>s</sub>) helps to establish appropriate PTFs to estimate K<sub>s</sub> indirectly from available soil basic properties. In doing so, we gathered an exhaustive list of soil chemical and physical properties which have been reported to be associated with soil K<sub>s</sub> for the predominant agroecological systems (Candemir and Gülser 2012). A pool of 16 soil basic properties was determined according to Oosterbaan and Nijland (1994) and Mbonimpa et al. (2002). Saturated hydraulic conductivity (K<sub>s</sub>) was measured on intact soil cores by the constant head method (Klute and Dirksen 1986). K<sub>s</sub> and all soil basic properties were analyzed on three replicate samples, and the average values were used in our experiment. The selected soil basic properties and the analytical protocols are presented in Table 1.

### 2.5 Calibration and validation of published PTFs

A variety of PTFs with different mathematical concepts, predicted hydraulic properties, and input data requirements have been developed. Physicoempirical methods by Tyler and Wheatcraft (1989) use the concept of shape similarity between pore and particle size distributions. The vast majority of PTFs, however, are empirically based on linear regression equations between hydraulic properties and soil basic properties. These PTFs can be categorized into three main groups including class PTFs, continuous PTFs, and neural networks (Schaap et al. 1999). All of these PTFs use at least some information about the particle size distribution, and considerable differences exist among PTFs in terms of the input soil data required. In our experiment, 12 sophisticated PTFs including Cosby, Brakensiek, Ahuja, Campbell, Puckett, Saxton, Vereecken, Rawls, CamShiozawa, Wösten1997, Wösten1999, and Li were introduced, and the appropriateness of these PTFs was evaluated using our dataset. The details of these PTFs were reported in existing literatures (Tietje and Tapkenhinrichs 1993; Wagner et al. 2001; Li et al. 2007).

In addition to the above 12 published PTFs, multiple linear regression (MLR), modified Vereecken (MV) model, and ANN were also adopted to establish PTFs using the same soil dataset. A stepwise regression was performed in the MLR using K<sub>s</sub> as dependent variable and 16 soil basic properties as independent variables, and the model having the highest accuracy and least input data was determined as the optimal PTF. MV PTF added EC<sub>e</sub> into input soil data compared with the well-known Vereecken PTF. Therefore, five soil basic properties including B<sub>d</sub>, S<sub>A</sub>, SOM, EC<sub>e</sub>, and C<sub>L</sub> were used

**Fig. 2** Description of vegetation type and the horizonation of representative soil pits



as input data in the MV PTF. The above five soil basic properties were also used as input soil data in the ANN PTF.

Two different procedures have been commonly used for the validation of PTF models. The first is a traditional method using statistical comparison between measured and predicted K<sub>s</sub> values. The second approach is a process-based functional validation using the soil hydraulic parameters to predict water flow with the software program (Simunek et al. 1998). The first procedure was adopted in our study. In doing so, K<sub>s</sub> and

soil basic properties at 84 sampling sites were randomly selected from our total dataset as calibration dataset, and K<sub>s</sub> and soil basic properties at the rest 40 sampling sites were used as validation dataset. Using the calibration dataset, the parameters of above 12 sophisticated PTFs were refitted, and the reliability of these refitted PTFs was tested based upon the validation dataset. To assess the calibration and validation performance of these PTFs, four criteria were considered: (i) the mean relative error (MRE), (ii) the root mean square error

**Table 1** The selected soil basic properties and the analytical protocols

Factor	Soil basic property	Protocol	Reference
Physical factor	Content of sand particles, S <sub>d</sub>	Bouyoucos hydrometer method	Bouyoucos (1962)
	Content of silt particles, S <sub>l</sub>		
	Content of clay particles, C <sub>l</sub>		
	Bulk density, B <sub>d</sub>	Core method	Blake and Hartge (1986)
	Total porosity, T <sub>Por</sub>	Core method	Marshall and Holmes (1988)
	Effective porosity, E <sub>Por</sub> <sup>a</sup>	–	Yu et al. (1993)
	Saturated water content, θ <sub>s</sub>	Water saturation method	Shahi (1968)
	Field capacity, θ <sub>fc</sub>	Wilcox method	Salter and Williams (1965)
Wilting point, θ <sub>w</sub> <sup>b</sup>	–	Wang and Schmutge (1980)	
Chemical factor	Electrical conductivity, EC <sub>e</sub>	Saturated soil paste extract	U.S. Salinity Laboratory Staff (1954)
	Sodium adsorption ratio, SAR <sub>e</sub> <sup>c</sup>	Saturated soil paste extract	Jurinak and Suarez (1990)
	Soil organic matter, SOM	Modified Walkley-Black	Nelson and Sommer (1982)
	Total nitrogen, TN	Kjeldah	Bremner (1960)
	Available nitrogen, AN	Alkaline hydrolysis diffusion	Cornforth and Walmsley (1971)
	Available phosphate, AP	Sodium bicarbonate Olsen method	Pierzynski (2000)
	Available potassium, AK	Flame photometric method	Motsara and Roy (2008)

<sup>a</sup> Effective porosity (E<sub>Por</sub>) is determined by T<sub>Por</sub> - θ<sub>fc</sub>, where T<sub>Por</sub> is the total porosity (cm<sup>3</sup>/cm<sup>3</sup>), θ<sub>fc</sub> is the volumetric water content at field capacity (cm<sup>3</sup>/cm<sup>3</sup>)

<sup>b</sup> Wilting point (W<sub>p</sub>) is calculated by (0.06774 - 0.00064 × S<sub>d</sub> + 0.00478 × C<sub>l</sub>) × B<sub>d</sub>, where S<sub>d</sub> is the gravimetric content of sand (%), C<sub>l</sub> is the gravimetric content of clay (%), B<sub>d</sub> is the bulk density (g/cm<sup>3</sup>)

<sup>c</sup> SAR<sub>e</sub> is computed as Na<sup>+</sup> / √(Ca<sup>2+</sup> + Mg<sup>2+</sup>) / 2, where Na<sup>+</sup>, Ca<sup>2+</sup>, Mg<sup>2+</sup> = measured water-soluble content of Na<sup>+</sup>, Ca<sup>2+</sup>, and Mg<sup>2+</sup> in saturated soil paste extract, respectively

(RMSE), (iii) the coefficient of determination ( $R^2$ ), and (iv) Akaike's information criterion (AIC). These criteria (Burnham and Anderson 2004) were defined as follows:

$$MRE = \frac{1}{n} \sum_{i=1}^n \frac{(P_i - M_i)}{M_i} \times 100\% \quad (1)$$

$$RMSE = \sqrt{\frac{1}{n} \sum_{i=1}^n (P_i - M_i)^2} \quad (2)$$

$$R^2 = \left[ \frac{\sum_{i=1}^n (M_i - \bar{M})(P_i - \bar{P})}{\left[ \sum_{i=1}^n (M_i - \bar{M})^2 \right]^{0.5} \left[ \sum_{i=1}^n (P_i - \bar{P})^2 \right]^{0.5}} \right]^2 \quad (3)$$

$$AIC = 2p + n \ln \left( \sum_{i=1}^n (P_i - M_i)^2 \right) \quad (4)$$

where  $n$  is the number of observations,  $P_i$  and  $M_i$  are the  $i$ th model calibrated (estimated) and measured values ( $i=1, 2, \dots, n$ ), and  $\bar{P}$  and  $\bar{M}$  are the calibrated (estimated) and measured mean values, respectively.  $p$  is the number of parameters used in the PTFs. For good fitness,  $MRE$  should be close to 0 and  $R^2$  close to 1, and  $RMSE$  and  $AIC$  parameters should be as low as possible.

## 2.6 Statistical analysis

To determine the influencing factors of soil  $K_s$ , factor analysis was used to reduce the entire dataset by grouping the 16 variables (soil basic properties) with SPSS software. Principal component analysis was used as the method of factor extraction in our study as it does not require prior estimates of the variation in each variable (Webster and Oliver 1990). Using a correlation matrix, principal component analysis was performed on the standardized soil basic properties with each property having a zero mean and unit variance (Riitters et al. 1995). Only factors with eigenvalues  $>1$  were retained and subjected to varimax rotation to maximize correlation between factors and measured variables. Communalities estimated the proportion of the variance in each soil property explained by

the components, and a high communality estimate suggested that a high portion of variance was explained by the factor.

The calibration dataset was used to refit the selected PTFs, and this was done with the help of nonlinear fitting tool in the environment of OriginPro 8.5. The Levenberg-Marquardt algorithm based upon nonlinear least squares was used, and the parameters in each PTF were optimized until the fitting converged, i.e., the tolerance criterion ( $1E-9$ ) with the maximum iteration number of 400 was satisfied. A neural network approach was also established to estimate  $K_s$  from soil basic properties. The detailed principle and procedure of neural networks are referred to Sharma et al. (2003). A back-propagation ANN with one input layer, one hidden layer, and one output layer was chosen in our study. The number of hidden nodes depended on the complexity of the underlying problem and was determined empirically by calibrating neural networks with different numbers of hidden nodes (Schaap and Leij 1998). This was done by separating the calibration dataset (84 sampling sites) into the training dataset (64 sampling sites) and the cross-validation dataset (20 sampling sites), and calibrating the neural network on the training dataset and subsequently testing the network on the cross-validation dataset. The training, testing, and validation of neural network were performed using the neural network toolbox of MATLAB 7.0.

## 3 Results

### 3.1 Profile characterization of $K_s$

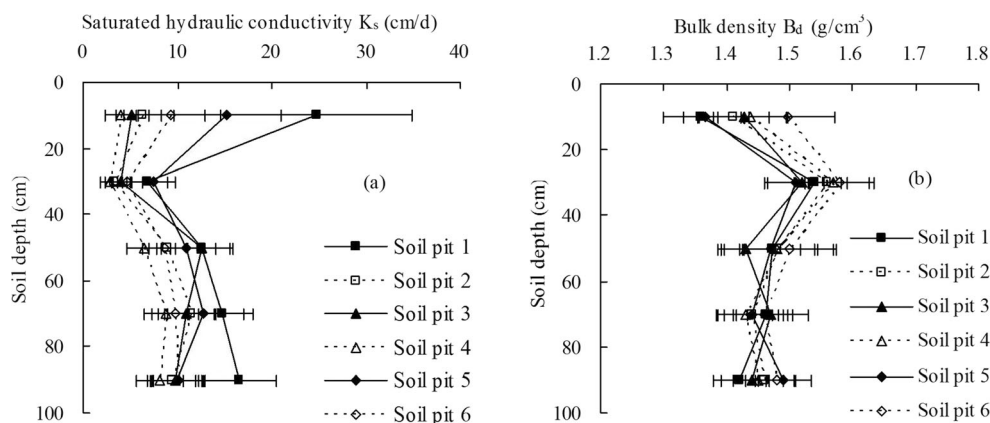
The profile characterization of soil  $K_s$  is presented in Fig. 3 (left graph). It can be seen that  $K_s$  generally exhibited valley distribution in the soil profile, decreasing with soil depth at 0–40-cm layer and increasing with soil depth at 40–100-cm layer. It also showed that 20–40-cm soil layer (Ap2 horizon) had the lowest  $K_s$  value ranging between 2.75 and 6.73 cm/day. It was interesting to find that substratum (40–100 cm) had higher  $K_s$  values than surface layer in some soil pits such as soil pit 3 and soil pit 4.

Severe soil compaction was observed in the profile distribution of bulk density in Fig. 3 (right graph). Due to the presence of plow pan, Ap2 horizon had the highest bulk density with an average of 1.55 g/cm<sup>3</sup> whereas the average bulk density at Ap1 and C horizons was 1.42 and 1.46 g/cm<sup>3</sup>, respectively.

### 3.2 Descriptive statistics of soil $K_s$ and basic properties

The descriptive statistics of soil  $K_s$  and basic properties for calibration dataset, validation dataset, and all sampling sites are shown in Table 2. The soil  $K_s$  ranged between 1.37 and

**Fig. 3** Characterization of saturated hydraulic conductivity and bulk density in typical soil pits



54.13 cm/day with an average of 11.41 cm/day for all samples across our experimental sites. Two textural classes were observed for all soil samples, and silty loam was determined as the predominant textural class. The average bulk density was  $1.42 \text{ g/cm}^3$  with soil porosity ranging from 0.40 to  $0.55 \text{ cm}^3/\text{cm}^3$ . The effective porosity which contributed to the water flow of saturated soil varied between  $0.09$  and  $0.27 \text{ cm}^3/\text{cm}^3$ , and the mean effective porosity was  $0.17 \text{ cm}^3/\text{cm}^3$ . Representing the water retention characteristics,  $\theta_w$ ,  $\theta_{fc}$ , and  $\theta_s$  had mean values of 0.16, 0.29, and  $0.39 \text{ cm}^3/\text{cm}^3$ , respectively, and this indicated that the plant available water capacity was  $0.13 \text{ cm}^3/\text{cm}^3$ . When considering the saline and alkali indices of soil, the average soil salinity was 10.03 dS/m, and SAR varied from 0.15 to 9.46 with an average of 2.32. With regard to the soil fertility indices, the mean SOM, TN, AN, AP, and AK were 7.82 g/kg, 0.51 g/kg, 71.95 mg/kg, 40.65 mg/kg, and 226.84 mg/kg, respectively.

### 3.3 Grouping of soil basic properties

Correlation analysis among  $K_s$  and 16 soil physical and chemical attributes resulted in significant correlation ( $P \leq 0.05$ ) among 93 of the 136 variable pairs (Table 3). This indicated that soil basic properties can be grouped into factors based on their correlation patterns.  $K_s$  had significant correlation with almost soil basic properties except  $C_L$ , AN, AP, and AK. High positive correlations were observed between  $K_s$  and  $E_{por}$ ,  $C_L$  and  $\theta_w$ ,  $T_{por}$  and  $E_{por}$ ,  $T_{por}$  and  $\theta_s$ ,  $EC_e$  and SAR, and SOM and TN ( $r \geq 0.70$ ). Strongest negative correlations were obtained between  $B_d$  and  $E_{por}$  ( $r \geq 0.90$ ),  $S_A$  and  $\theta_{fc}$  ( $r \geq 0.80$ ),  $S_A$  and  $S_I$ , and  $B_d$  and  $\theta_s$  ( $r \geq 0.70$ ).  $C_L$ ,  $B_d$ , SOM, and TN had significant correlations with the largest number of other soil properties.

Rotated component loadings and communality estimates for all soil basic properties are shown in Table 4. The first five PCs had eigenvalues  $>1$  and accounted for 91.05 % of variance in measured soil properties and therefore were retained

for further interpretation. Communalities for all soil basic properties indicated that the five factors explained  $>95$  % of variance in  $S_A$ ,  $S_I$ ,  $C_L$ ,  $B_d$ ,  $T_{por}$ ,  $E_{por}$ ,  $\theta_s$ ,  $\theta_{fc}$ , and  $\theta_w$ ;  $>90$  % of variance in  $EC_e$ , SAR, and SOM;  $>80$  % of variance in TN. However, the five components explained  $<70$  % of variance in AN, AP, and AK (Table 4). Thus, AN, AP, and AK were considered to be the least important soil properties due to the lowest communality estimates.

The order by which the principal components (PCs) were interpreted was determined by the magnitude of their eigenvalues. The first PC explained 40.02 % of the variance (Table 4). It had high positive loadings from  $T_{por}$  (0.95),  $E_{por}$  (0.86), and  $\theta_s$  (0.88), and negative loading from  $B_d$  (−0.95). PC1 was identified as the “soil porosity component” since it mainly explained variations in characters related to soil bulk density and porosity status. The second PC explained 20.38 % of the variance with high positive loadings from  $S_A$  (0.97) and  $\theta_s$  (0.88), and high negative loadings from  $S_I$  (−0.88) and  $\theta_{fc}$  (−0.96). We named PC2 “water retention component” because all soil properties comprised in this component were significantly correlated ( $p < 0.05$ ) with  $\theta_s$  and  $\theta_{fc}$  (Table 4). The third PC was called “organic matter component.” It explained 13.51 % of the variance with high positive loading from SOM (0.84), TN (0.83), and AN (0.80) and moderate loadings from AP (0.64) and AK (0.60). These properties were indicators of soil organic matter and were significantly correlated (Table 4). Explaining 9.04 % of the variance, the PC4 was termed “soil salinity component.” It had high positive loading for  $EC_e$  (0.92) and SAR (0.93). Neither high positive nor moderate negative loading was found for the fourth PC. This showed that soil salinity was also an important influencing factor of soil  $K_s$ . The fifth PC explained 8.10 % of the variance and was referred to as “unavailable water component” as it had high positive loading from  $\theta_w$  (0.94), and this property represented the soil water content at which crop root could not uptake due to excessively high soil water suction. PC5 also had high positive loading from  $C_L$  (0.88).

**Table 2** Descriptive statistics of  $K_s$  and soil basic properties for calibration dataset, validation dataset, and all sampling sites

Dataset	Index	$K_s$	Soil physical properties										Soil chemical properties						
			$S_A$	$S_I$	$C_L$	$B_d$	$T_{por}$	$E_{por}$	$\theta_s$	$\theta_{fc}$	$\theta_w$	$EC_e$	$SAR$	$SOM$	$TN$	$AN$	$AP$	$AK$	
Total datasets ( $n=124$ )	Min.	1.37	8.37	50.31	7.20	1.21	0.40	0.09	0.35	0.27	0.13	1.28	0.15	1.17	0.10	6.22	1.65	64.76	
	Max.	54.13	33.69	82.16	19.09	1.60	0.55	0.27	0.44	0.31	0.21	29.59	9.46	18.50	1.30	176.57	146.38	808.82	
	Mean	11.41	19.92	67.20	12.88	1.42	0.47	0.17	0.39	0.29	0.16	10.03	2.32	7.82	0.51	71.95	40.65	226.84	
	St. d.	8.43	19.71	67.37	13.12	1.42	0.47	0.17	0.39	0.29	0.16	8.18	1.85	7.63	0.50	69.96	36.97	206.00	
	$C_v$ (%)	9.85	5.78	7.64	3.03	0.07	0.03	0.03	0.03	0.02	0.01	6.11	1.72	2.67	0.19	33.86	25.70	100.26	
Calibration dataset ( $n=84$ )	Min.	1.37	9.99	50.73	7.20	1.21	0.40	0.09	0.35	0.27	0.13	1.28	0.15	1.17	0.10	6.22	1.65	64.76	
	Max.	54.13	33.12	80.63	19.09	1.60	0.55	0.27	0.42	0.31	0.21	27.76	9.46	18.50	1.30	176.57	146.38	808.82	
	Mean	11.50	19.81	67.38	12.81	1.41	0.47	0.17	0.39	0.29	0.16	10.27	2.39	7.73	0.51	71.87	40.30	228.42	
	St. d.	10.31	5.56	7.31	3.07	0.08	0.03	0.03	0.02	0.01	0.02	6.14	1.80	2.90	0.21	35.02	26.04	109.32	
	$C_v$ (%)	89.65	28.09	10.84	23.99	5.38	6.16	19.45	4.19	3.14	12.53	59.77	74.99	37.54	40.90	48.72	64.62	47.86	
Validation dataset ( $n=40$ )	Min.	1.98	8.37	50.31	7.77	1.24	0.40	0.09	0.36	0.27	0.13	2.09	0.25	3.77	0.22	12.88	3.42	109.00	
	Max.	39.77	33.69	82.16	18.23	1.59	0.53	0.23	0.44	0.31	0.21	29.59	7.49	13.06	0.86	142.41	126.99	488.44	
	Mean	11.23	20.15	66.82	13.03	1.42	0.47	0.17	0.39	0.29	0.17	9.51	2.16	8.00	0.51	72.13	41.39	223.53	
	St. d.	8.95	6.28	8.37	2.97	0.07	0.03	0.03	0.02	0.01	0.02	6.08	1.56	2.12	0.14	31.71	25.28	79.05	
	$C_v$ (%)	79.64	31.16	12.53	22.77	4.99	5.75	17.74	4.51	3.41	11.41	63.90	72.32	26.48	28.11	43.96	61.08	35.37	

**Table 3** Correlation among  $K_s$  and soil basic properties (based on all 124 sampling sites)

$K_s$	$S_A$	$S_I$	$C_L$	$B_d$	$T_{por}$	$E_{por}$	$\theta_s$	$\theta_{fc}$	$\theta_w$	$EC_e$	$SAR$	$SOM$	$TN$	$AN$	$AP$
$S_A$	0.462**														
$S_I$	-0.221*	-0.721**													
$C_L$	0.164	0.379**	-0.609**												
$B_d$	-0.693**	-0.413**	0.391**	-0.182*											
$T_{por}$	0.693**	0.413**	-0.391**	0.182*	-1.000**										
$E_{por}$	0.726**	0.622**	-0.589**	0.275**	-0.967**	0.967**									
$\theta_s$	0.443**	-0.169	0.044	0.201*	-0.783**	0.783**	0.628**								
$\theta_{fc}$	-0.466**	-0.861**	0.411**	-0.426**	0.381**	-0.381**	-0.605**	0.168							
$\theta_w$	-0.245**	-0.049	-0.313**	0.834**	0.343**	-0.343**	-0.288**	-0.084	-0.024						
$EC_e$	-0.365**	-0.157	0.212*	-0.183*	0.495**	-0.495**	-0.466**	-0.425**	0.145	0.073					
$SAR$	-0.301**	-0.156	0.211*	-0.192*	0.357**	-0.357**	-0.348**	-0.289**	0.144	0.017	0.843**				
$SOM$	0.481**	0.194*	-0.147	0.350**	-0.522**	0.522**	0.550**	0.367**	0.025	-0.647**	-0.561**	0.808**			
$TN$	0.221*	0.156	-0.061	0.452**	-0.364**	0.364**	0.398**	0.263**	0.205*	-0.530**	-0.481**	0.554**	0.808**		
$AN$	-0.103	0.107	-0.135	0.420**	-0.073	0.073	0.114	0.059	0.338**	-0.289**	-0.284**	0.724**	0.724**		
$AP$	0.169	0.140	-0.117	0.320**	-0.103	0.103	0.132	0.112	0.171	-0.159	-0.171	0.508**	0.705**	0.606**	
$AK$	0.156	0.111	-0.112	0.473**	-0.202*	0.202*	0.167	0.173	0.140	-0.217*	-0.188*	0.621**	0.710**	0.561**	0.585**



**Table 4** Rotated component loadings and communality estimates for all soil basic properties

Soil basic property	PC1	PC2	PC3	PC4	PC5	Communalities
$S_A$	0.11	0.97	0.18	-0.09	0.03	0.990
$S_I$	-0.14	-0.88	-0.23	0.11	-0.37	0.993
$C_L$	0.14	0.37	0.24	-0.11	0.88	0.997
$B_d$	-0.95	-0.21	-0.10	0.17	0.11	0.996
$T_{por}$	0.95	0.21	0.10	-0.17	-0.11	0.995
$E_{por}$	0.86	0.46	0.13	-0.17	-0.07	0.996
$\theta_s$	-0.42	0.88	0.05	-0.14	0.12	0.991
$\theta_{fc}$	-0.11	-0.96	-0.14	0.07	-0.10	0.971
$\theta_w$	-0.29	0.03	0.16	-0.01	0.94	0.996
$EC_e$	-0.24	-0.06	-0.12	0.92	-0.02	0.926
$SAR$	-0.14	-0.08	-0.11	0.93	-0.08	0.907
$SOM$	0.27	0.25	0.84	-0.30	0.00	0.936
$TN$	0.18	0.18	0.83	-0.24	0.09	0.813
$AN$	-0.06	0.07	0.80	-0.05	0.17	0.677
$AP$	0.02	0.07	0.64	-0.03	0.03	0.413
$AK$	0.16	0.19	0.60	0.04	0.17	0.454
						Total
Eigenvalue	6.40	3.26	2.16	1.45	1.30	–
Difference	3.14	1.10	0.72	0.15	0.83	–
% of variance explained	40.02	20.38	13.51	9.04	8.10	91.05

### 3.4 Appropriateness assessment of published PTFs

Results of calibration and validation criteria of 12 selected PTFs are presented in Table 5. According to the calibration criteria, all the selected PTFs exhibited satisfactory calibration performance except for Cosby, Puckett, and CamShiozawa PTFs. This was not unexpected considering that the influencing properties of  $K_s$  were grouped into five soil factors and only soil texture was used as input data in these PTFs. When considering the validation criteria, the estimation performance of each PTF varied greatly, and all the PTFs overestimated  $K_s$

**Table 5** Accuracy of calibration and validation of all selected PTFs

PTFs	Calibration criteria				Validation criteria			
	MRE (%)	RMSE	R <sup>2</sup>	AIC	MRE (%)	RMSE	R <sup>2</sup>	AIC
Cosby	68.874	8.818	0.261	371.70	67.645	7.718	0.147	167.48
Brakensiek	19.223	5.729	0.693	299.25	25.116	6.206	0.469	152.04
Ahuja	34.753	6.435	0.606	314.78	37.431	5.552	0.503	139.13
Campbell	41.772	6.552	0.592	321.81	43.752	5.737	0.464	145.76
Puckett	81.992	10.116	0.026	390.78	80.567	7.628	0.064	164.55
Saxton	31.980	6.382	0.613	317.38	47.250	7.509	0.333	167.29
Vereecken	38.671	6.490	0.599	322.21	39.941	5.510	0.497	144.52
Rawls	24.770	5.918	0.670	304.72	31.494	6.964	0.421	161.26
CamShiozawa	68.874	8.818	0.261	369.70	67.646	7.718	0.147	167.48
Wösten1997	25.220	5.810	0.681	301.61	35.759	7.491	0.392	167.10
Wösten1999	24.524	5.835	0.679	304.33	38.498	6.147	0.461	153.28
Li	28.870	5.968	0.663	310.13	35.732	6.112	0.455	154.82

regarding to MRE parameter. Ahuja PTF generally had the best estimation performance with the least RMSE and AIC parameters, indicating that effective porosity could be used as an estimation of soil  $K_s$  in our experimental sites. Vereecken PTF also exhibited satisfactory estimation performance, and the possible reason was that  $S_A$ ,  $C_L$ , SOM, and  $B_d$  representing four influencing factors of  $K_s$  were used as input data in this PTF.

### 3.5 Evaluation on the established PTFs

#### 3.5.1 Multiple linear regression

The statistics of MLR analysis suggested that the highest accuracy was obtained when using  $E_{Por}$ , SOM, and AN as predictors. Including other soil basic properties did not result in significant improvement of  $K_s$  prediction. Refitting the equation with  $E_{Por}$ , SOM, and AN as predictors yielded:

$$K_s = 172.116E_{Por} + 1.274SOM - 0.113AN - 20.581 \quad (5)$$

The calibration and validation criteria of MLR PTF are shown in Table 6. Apparently, this PTF had the least MRE parameter, i.e., the least prediction bias, and this could be ascribed to the nature of unbiased estimate of linear regression method. With respect to prediction performance, the validation criteria of MLR PTF were similar to those of Ahuja and Vereecken PTFs, and the prediction accuracy of MLR PTF was also satisfactory.

#### 3.5.2 Modified Vereecken model

With Levenberg-Marquardt algorithm, the nonlinear fitting was employed to fit the MV PTF using the calibration dataset. The obtained MV PTF was given by

**Table 6** Accuracy of calibration and validation of the established PTFs

PTFs	Calibration criteria				Validation criteria			
	MRE (%)	RMSE	R <sup>2</sup>	AIC	MRE (%)	RMSE	R <sup>2</sup>	AIC
MLR	13.958	6.291	0.630	314.98	21.432	5.623	0.515	143.33
MV	36.776	6.227	0.632	313.25	40.411	5.236	0.546	141.65
ANN	13.744	5.986	0.673	310.62	19.030	4.871	0.621	136.67

$$K_s = 4.540 \times 10^{-5} \cdot \exp(21.646 - 0.197 \cdot \ln(C_L) + 0.414 \cdot \ln(S_A) - 0.078 \cdot \ln(SOM) - 6.982 \cdot B_d - 0.006 \cdot EC_e) \quad (6)$$

When comparing Tables 5 and 6, it can be seen that the RMSE and AIC parameters of MV PTF were lower than those of Vereecken PTF, indicating that MV PTF had better calibration performance than Vereecken PTF, and it was also the case for prediction capability. Therefore, the established MV PTF, in which the effect of soil salinity on K<sub>s</sub> was considered, was more suitable for the coastal salt-affected soil than the commonly used Vereecken PTF.

### 3.5.3 Artificial neural network

In order to prevent the “overtraining” of neural network, the number of hidden nodes was optimized using trial and error method. In doing so, the input layer and output layer of ANN PTF were maintained using the same nodes, increasing the hidden nodes from 5 to 17 resulted in variation in training error (RMSE) and cross-validation error (Fig. 4). The training error generally decreased with the increasing hidden nodes whereas cross-validation error increased with hidden nodes. From Fig. 4, when hidden nodes increased to 8, the network had the optimal performance, i.e., the least cross-validation

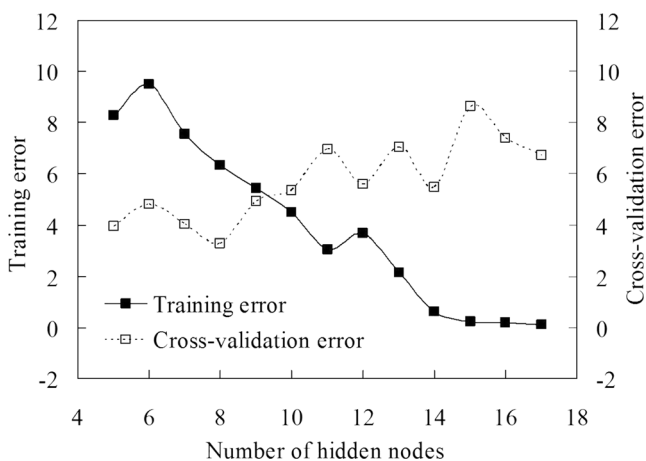


**Fig. 4** Training error and check error related to number of hidden nodes in the artificial neural network

error. Therefore, the nodes in input layer, hidden layer, and output layer of ANN were fixed to 5, 8, and 1, respectively.

Using the above ANN PTF, the training dataset, cross-validation dataset, and testing dataset were simulated and presented in Fig. 5. Table 6 also shows the calibration and validation criteria of ANN PTF. Compared with MLR and MV PTFs, the ANN PTF had the best prediction accuracy owing to the least MRE, RMSE, and AIC parameters and highest R<sup>2</sup> parameter.

## 4 Discussion

### 4.1 Characteristics of K<sub>s</sub> in different soil horizons

Saturated hydraulic conductivity (K<sub>s</sub>) in the soil profile was classified as low permeability according to Bhattacharyya et al. (2008), and the lowest K<sub>s</sub> was observed at the Ap2 horizon (20–40-cm layer). This is consistent with the finding of Wang et al. (2011) who also found that soil K<sub>s</sub> exhibited the trend of decreasing at subsurface layer (20–40 cm) and

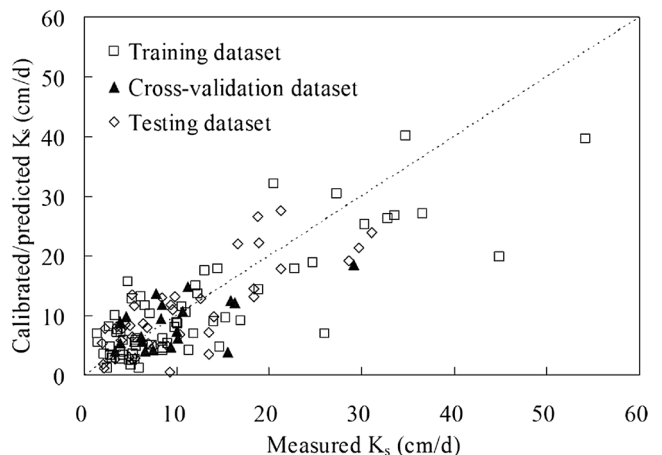


**Fig. 5** Scatter plots of the measured versus calibrated/predicted K<sub>s</sub> values

increasing at substratum (40–100 cm) for salt-affected soils in the coastal farming area. This phenomenon was not unexpected considering that 20–40-cm layer was the traditional plough pan for the cultivated soil and tillage measures resulted in the mechanical compaction at 20–40-cm layer. This is supported by the difference of the contents of soil particles between Ap1 and Ap2 horizons in each soil pit (Fig. 2). The possible reason for higher  $K_s$  values at substratum than surface layer (such as soil pit 3 and soil pit 4) is that at these sites, soil surface was barren due to high soil salinity which exceeded the common salt tolerance level of maize, and barren soil surface generally resulted in soil aggregate breakdown and soil compaction in comparison with vegetation coverage condition (Engelaar et al. 2000).

In addition to particle size distribution, bulk density was the most widely used soil property in assessing soil hydraulic conductivity in most literatures. Our results showed that the profile characterization of bulk density was generally opposite to that of  $K_s$ . This was not surprising as bulk density representing the total porosity status was closely related to soil permeability.  $K_s$  was reported to decrease with bulk density for most important soil series (Wang et al. 2003). Dec et al. (2008) found that the hydraulic properties of soils with identical texture depended on bulk density and structure. The finding of Assouline (2006) showed that the Kozeny equation with sole information on the bulk density could be used successfully to predict the saturated hydraulic conductivity for both compacted and uncompact soils. In this study, the average  $K_s$  was generally below the measured values for silty loam soils as reported by Fuentes et al. (2004), Fuentes and Flury (2005), and Li et al. (2007), and this could be ascribed to higher soil compaction and lower porosity in our experimental sites.

#### 4.2 Principal components of basic properties affecting soil $K_s$

Our finding showed that the basic soil properties of  $K_s$  could be grouped into five factors, i.e., soil porosity, water retention capacity, organic matter, soil salinity, and unavailable water content. This coincided with Wang et al. (2011) who found that soil porosity, texture, and salinity were important influencing factors of coastal soil  $K_s$  in the similar region. However, the conclusion was different for soil  $K_s$  at other regions. Candemir and Gülser (2012) stated that exchangeable Na had the highest direct effect on  $K_s$  and exchangeable Na was one of the most important soil properties that affected  $K_s$  directly in fine-textured alkaline soils. Li et al. (2008) showed that soil texture and porosity had significant influences on  $K_s$  in southwest Karst region of China. For the typical farmland in the red soil area, soil porosity, organic matter, and soil texture were determined as important influencing factors of  $K_s$  (Fang et al. 2008). As expected, soil porosity, texture, and organic matter were the most frequently used factors of soil  $K_s$  in most

existing literatures. Our study also showed that soil salinity had adverse impact on  $K_s$  of the coastal farmland, indicating that soil salinity played an important role in the estimation of  $K_s$  when using PTFs. The reasons included the following: (i) substantial exchangeable  $Na^+$  in the coastal farmland resulted in dispersed silt and clay particles and soil pore clogging and (ii) high soil salinity inhibited crop growth and root intersperse which contributed to improvement of soil permeability.

The influencing factors of agricultural soil  $K_s$  vary, depending on not only the nature of soil such as soil type, texture, porosity, pore connectivity, and organic matter, but also the management practices used such as land use, tillage, and irrigation water quality. Based upon a new global database of field hydraulic conductivity, Jarvis et al. (2013) found that topsoil  $K_s$  depended more strongly on bulk density, organic carbon content, and land use but weakly on texture. Organic carbon showed negative correlation with  $K_s$  because of water repellency and  $K_s$  at arable sites was, on average, two to three times smaller than under natural vegetation, forests, and perennial agriculture. In a recent study by Reading et al. (2012),  $K_s$  was found to increase in a sodic clay soil in response to gypsum applications, and a suggestion was proposed that sodium needed to be taken into account when determining the suitability of water quality for irrigation of sodic soils. This showed agreement with Yasin et al. (1989) who stated that increasing soil exchangeable sodium percentage (ESP) resulted in a constant decrease in soil  $K_s$  and irrigation water with high sodium adsorption ration (SAR) and residual sodium carbonate (RSC) significantly reduced soil  $K_s$ .

#### 4.3 Effect of soil type and measuring methods on the selection of PTFs

Much attention has been paid to the comparison of PTFs by many authors (Wagner et al. 2001; Stumpp et al. 2009), but the conclusion is essentially the same: There is no PTF that is the most suitable for all soils, but rather a toolbox of alternative methods from which to choose or to conduct the method best suited for the soil at hand. In this study, the estimation capability of Saxton and Wösten1997 PTFs were found inferior to that of Brakensiek, Campbell, Rawls, Wösten 1999, or Li PTFs. The explanation was that soil porosity was not employed in the Saxton PTF, and soil properties of water retention capacity were not used in the Wösten1997 PTF. Generally, Ahuja and Vereecken PTFs showed the best appropriateness for soil  $K_s$  estimation in the coastal reclamation farming area, and Ahuja PTF was identified as the most convenient method as only effective porosity was needed in this PTF. This was also found by Aimrun et al. (2004) who estimated paddy soil  $K_s$  from effective porosity data with success. In another rigorous study, Tietje and Tapkenhinrichs (1993) made an exhaustive comparison between the well-known PTFs and drew a conclusion that

Vereecken PTF was considered the best and applicable for all soil samples, even for high organic matter contents. This summarization showed agreement with the results of our statistical analysis. As a matter of fact, the accuracy of PTFs varies with different soil types, scale of soil sampling, measurement methods, as well as textural classes. According to Tietje and Tapkenhinrichs (1993) and Wagner et al. (2001), Rawls PTF had no advantage for predicting sandy soils whereas Puckett PTF might be applied only in sandy soils, and Saxton PTF generally underestimated for soils with high organic carbon content. Earlier studies showed that Wösten1999 and Li PTFs were more applicable in the area of fluvo-aquic soils in Fengqiu County (Li et al. 2009). Rawls PTF exhibited the best performance in soil  $K_s$  estimation in the tianran wenyanqu Basin of Huang-Huai-Hai Plain (Li et al. 2010) whereas Zhang et al. (2010) suggested Cosby PTF as the best method for paddy soils in the lower Yangtze River Delta. As must be noted that, in the evaluation of PTFs, all samples must be measured using the same method, i.e., attention should also be paid to the homogeneity of the soil data. Results of Tietje and Hennings (1996) showed that Vereecken PTF derived from large measurement volume obviously led to poor results when it is applied to data collected by another method. In our study, core and bulk soil samples were collected from the two experimental sites using the same method, and soil samples were analyzed by the identical approaches. When compared to the result of Cosby et al. (1984) with Tietje and Hennings (1996), it was found that the involved textural classes of soil samples were also associated with the prediction performance of PTFs.

#### 4.4 The advantage of artificial neural network in developing PTFs

As expected, the developed ANN PTF had the best prediction performance than the 12 well-known PTFs and MLR and MV PTFs. This was due to the fact that nonlinear information between  $K_s$  and soil basic properties was used in the neural network, whereas this information was absent in PTFs based upon linear regressions. This resulted in better prediction capability of neural network than linear regression provided that the same input soil data was used. Li et al. (2010) found that ANN PTF based upon Wösten 1997 had the best prediction precision for the fluvo-aquic soil in the tianran wenyanqu Basin. ANN-based PTFs also had better behavior in comparison with published program such as Rosetta and HYPRES. Parasuraman et al. (2006) evaluated the performance of field-scale ANN PTFs and Rosetta and found that the field-scale ANN PTFs performed better than Rosetta for the same dataset, and the ANN PTF employing the boosting algorithm resulted in better generalization by reducing both the bias and variance. In another study by Minasny et al. (2004), the neural network PTF using multistep outflow data reduced about

50 % prediction error when compared with predicted hydraulic functions using Rosetta. Based upon the complete soil water retention curve (SWRC) dataset, Li et al. (2007) compared three sets of existing PTFs, i.e., Vereecken, Rosetta, and HYPRES, with the developed PTF, and concluded that the proposed PTF did a better job in estimating the soil hydraulic parameters than the existing PTFs. In our study, Rosetta was not employed as a reference method to take part in the statistical comparison with various reasons. For one thing, only soil sand, silt and clay content, and bulk density (SSCBD) were used as input soil data in Rosetta considering our dataset, while the prediction accuracy generally increased if more input data are used (Schaap and Leij 1998). Thus, the ANN PTF as derived in our study privileged Rosetta in input data. For another, PTFs were developed on the basis of databases of a limited number of soil samples; consequently, they might not be directly applicable to soil conditions different than those under which they were developed (Nemes et al. 2003). The dataset used for constructing Rosetta was derived from soils in temperate to subtropical climates of North America and Europe, while the dataset of our study was established on coastal salt-affected soil which was reclaimed from mudflats with silty loam the predominant textural class. In other words, PTFs developed at a large scale were best suited for national or global modeling, but might be of little use on a farm field (Bastet et al. 1999).

## 5 Conclusions

In the coastal salt-affected farming area, soil  $K_s$  generally showed valley distribution in the soil profile and 20–40-cm soil layer (Ap2 horizon) had the lowest  $K_s$  value. Our experiment sites were characterized by low saturated hydraulic conductivity, coarse soil texture and soil porosity, low water retention capacity, high soil salinity, and deficit in soil nutrients. Using factor analysis, the 16 soil basic properties were grouped into five factors with 91.05 % of variance explained. The order of the five influencing factors was *soil porosity component, water retention component, organic matter component, soil salinity component, and unavailable water component*. Soil salinity had adverse impact on  $K_s$  of the coastal salt-affected farmland, and soil salinity played an important role in the estimation of  $K_s$  when using PTFs.

All the selected PTFs exhibited satisfactory calibration and prediction performance except Cosby, Puckett, and CamShiozawa PTFs. Among all selected PTFs, Ahuja and Vereecken PTFs showed the best appropriateness for soil  $K_s$  estimation in our experimental sites, and Ahuja PTF was identified as the most convenient method as only effective porosity was needed in this PTF, and Vereecken PTF was suited for a wider range of soil textural classes. Our established PTFs

showed better calibration and validation performance than the selected well-known PTFs. The MV PTF, which considered soil salinity in input soil data, was more suitable for the coastal salt-affected farmland. Using  $S_A$ ,  $C_L$ ,  $B_d$ , SOM, and  $EC_e$  as input soil data, the PTF based upon ANN was recommended as the best method to estimate soil  $K_s$  in our experimental sites.

The determination of influencing factors and appropriate PTF for soil saturated hydraulic conductivity remains more exploration, as agricultural soil  $K_s$  was affected by not only the nature of soil but also the field management practices, and to identify a universal PTF suitable for different soil types, scale of soil sampling, measurement methods as well as textural classes is impossible. The data used in this study belonged to only one crop season (maize/cotton) of our experimental sites as cultivated with the given two cropping systems just for 3–5 years only. Therefore, further efforts were needed to collect sufficient data and validate whether our suggested PTFs would be equally useful over time and scale, and in different management systems and land use patterns.

**Acknowledgments** This study was funded by the financial support of the National Natural Science Foundation of China (41101199; 41171181; 51109204), the Natural Science Foundation of Jiangsu Province (BK20141266), and the Key Technology R&D Program of Jiangsu Province (BE2014678). The authors wish to express cordial thanks to the staff of Jinhai Farm and Huanghai Raw Seed Growing Farm for assistant in soil sampling and field measurement. We also acknowledge the valuable comments of the anonymous reviewers.

## References

- Acutis M, Donatelli M (2003) SOILPAR 2.00: software to estimate soil hydrological parameters and functions. *European J Agr* 18:373–377
- Agyare WA, Park SJ, Vlek PLG (2007) Artificial neural network estimation of saturated hydraulic conductivity. *Vadose Zone J* 6:423–431
- Aimrun W, Amin MSM, Eltaib SM (2004) Effective porosity of paddy soils as an estimation of its saturated hydraulic conductivity. *Geoderma* 121:197–203
- Arrington KE, Ventura SJ, Norman JM (2013) Predicting saturated hydraulic conductivity for estimating maximum soil infiltration rates. *Soil Sci Soc Am J* 77:748–758
- Assouline S (2006) Modeling the relationship between soil bulk density and the hydraulic conductivity function. *Vadose Zone J* 5:697–705
- Bastet G, Bruand A, Voltz M, Bornand M, Quélin P (1999) Performance of available pedotransfer functions for predicting the water retention properties of French soils. In: van Genuchten MTh, Leij FJ (ed) *Characterization and measurement of the hydraulic properties of unsaturated porous media*. Proceedings of the International Workshop Riverside California, October 22–24, 1997, pp 981–992
- Bhattacharyya R, Kundu S, Pandey SC, Singh KP, Gupta HS (2008) Tillage and irrigation effects on crop yields and soil properties under the rice–wheat system in the Indian Himalayas. *Agr Water Manag* 95:993–1002
- Blake GR, Hartge KH (1986) Bulk density. In: Klute A (ed) *Methods of soil analysis*. Part I. Physical and Mineralogical Methods: Agronomy Monograph 9, pp 363–375
- Bouma J, Lanen JAJ (1987) Transfer functions and threshold values: from soil characteristics to land qualities. In: Beek KJ (ed) *Quantified land evaluation*. International Institute of Aerospace Survey Earth Science ITC publication 6, 106–110
- Bouyoucos GJ (1962) Hydrometer method improved for making particle size analysis of soils. *Agron J* 54:464–465
- Bremner JM (1960) Determination of nitrogen in soil by the Kjeldahl method. *J Agr Sci* 55:11–33
- Burnham KP, Anderson DR (2004) Multimodel inference: Understanding AIC and BIC in model selection. *Soc Method Res* 33:261–304
- Candemir F, Gülsler C (2012) Influencing factors and prediction of hydraulic conductivity in fine-textured alkaline soils. *Arid Land Res Manag* 26:15–31
- Cornelis WM, Ronsyn J, Van Meirvenne M, Hartmann R (2001) Evaluation of pedotransfer functions for predicting the soil moisture retention curve. *Soil Sci Soc Am J* 65:638–648
- Cornforth IS, Walmsley D (1971) Methods of measuring available nutrients in West Indian soils. *Plant and Soil* 35:389–399
- Cosby BJ, Hornberger GM, Clapp RB, Ginn TR (1984) A statistical exploration of the relationships of soil moisture characteristics to the physical properties of soils. *Water Resour Res* 20:682–690
- Dec D, Dörner J, Becker-Fazekas O, Horn R (2008) Effect of bulk density on hydraulic properties of homogenized and structured soils. *J Soil Sc Plant Nutr* 8:1–13
- Engelaar WMHG, Matsumaru T, Yoneyama T (2000) Combined effects of soil waterlogging and compaction on rice (*Oryza sativa* L) growth soil aeration soil N transformation and  $^{15}\text{N}$  discrimination. *Biol Fert Soils* 32:484–493
- Fang K, Chen XM, Zhang JB, Wang BR, Huang J, Gan ZF (2008) Saturated hydraulic conductivity and its influential factors of typical farmland in red soil region. *J Irri Drain* 27:67–69
- Franzmeier DP (1991) Estimation of hydraulic conductivity from effective porosity data for some Indiana soils. *Soil Sci Soc Am J* 55:1803–1891
- Fuentes JP, Flury M (2005) Hydraulic conductivity of a silt loam soil as affected by sample length. *Trans ASAE* 48:191–196
- Fuentes JP, Flury M, Bezdicek DF (2004) Hydraulic properties in a silt loam soil under natural prairie conventional till and no-till. *Soil Sci Soc Am J* 68:1679–1688
- Jarvis N, Koestel J, Messing I, Moeyes J, Lindahl A (2013) Influence of soil land use and climatic factors on the hydraulic conductivity of soil. *Hydrol Earth Syst Sci* 17:5185–5195
- Jurinak JJ, Suarez DL (1990) The chemistry of salt-affected soils and waters. In: Tanji KK (ed) *Agricultural Salinity Assessment and Management*. American Society of Civil Engineers, New York, p 42–63
- Klute A, Dirksen C (1986) Hydraulic conductivity and diffusivity: laboratory methods. In: Klute A (ed) *Methods of soil analysis*, part 1, physical and mineralogical methods, 2nd edn. ASA, Madison, WI, pp 687–734
- Lai JB, Ren L (2007) Assessing the size dependency of measured hydraulic conductivity using double-ring infiltrometers and numerical simulation. *Soil Sci Soc Am J* 71:1667–1675
- Lebron I, Schaap MG, Suarez DL (1999) Saturated hydraulic conductivity prediction from microscopic pore geometry measurements and neural network analysis. *Water Resour Res* 35:3149–3158
- Li Y, Chen D, White RE, Zhu A, Zhang J (2007) Estimating soil hydraulic properties of Fengqiu County soils in the North China Plain using pedo-transfer functions. *Geoderma* 138:261–271
- Li XL, Chen XM, Zhou LC, Fang K (2008) Soil saturated hydraulic conductivity and its influential factors in Southwest Karst region of China. *J Irri Drain* 27:74–76
- Li XP, Zhang JB, Ji LQ, Zhu AN, Liu JT (2009) Application of pedotransfer functions in calculating saturated soil hydraulic conductivity of Fengqiu County. *J Irri Drain* 28:70–73

- Li HX, Liu JL, Zhu AN, Zhang JH (2010) Comparison study of soil pedotransfer functions in estimating saturated soil hydraulic conductivity at Tianranwenyanqu Basin. *Soils* 42:438–445
- Lin HS, McInnes KJ, Wilding LP, Hallmark CT (1999) Effects of soil morphology on hydraulic properties: II hydraulic pedotransfer functions. *Soil Sci Soc Am J* 63:955–961
- Marshall TJ, Holmes JW (1988) *Soil physics*. Cambridge University Press, Cambridge, 374 pp
- Mbonimpa M, Aubertin M, Chapuis RP, Bussière B (2002) Practical pedotransfer functions for estimating the saturated hydraulic conductivity. *Geotech Geol Eng* 20:235–259
- Minasny B, Hopmans JW, Harter T, Eching SO, Tuli A, Denton MA (2004) Neural networks prediction of soil hydraulic functions for alluvial soils using multistep outflow data. *Soil Sci Soc Am J* 68: 417–429
- Motaghian HR, Mohammadi J (2011) Spatial estimation of saturated hydraulic conductivity from terrain attributes using regression kriging and artificial neural networks. *Pedosphere* 21:170–177
- Motsara MR, Roy RN (2008) *Guide to laboratory establishment for plant nutrient analysis*. Food and Agricultural Organization of the United Nations, Rome
- Nelson DW, Sommer LE (1982) Total carbon organic carbon and organic matter. In: Page AL (ed) *Methods of soil analysis*. Amer Soc Agron, Madison, WI, pp 539–579
- Nemes A, Schaap MG, Wösten JHM (2003) Functional evaluation of pedotransfer functions derived from different scales of data collection. *Soil Sci Soc Am J* 67:1093–1102
- Oosterbaan RJ, Nijland HJ (1994) Determining the saturated hydraulic conductivity. In: Ritzema HP (ed) *Drainage principles and applications*. International Institute for Land Reclamation and Improvement (ILRI), Publication 16, second revised edition, 1994, Wageningen, The Netherlands
- Pachepsky YA, Rawls WJ (2004) *Development of pedotransfer functions in soil hydrology*, Dev Soil Sci, 30 Elsevier Amsterdam
- Parasuraman K, Elshorbagy A, Si BC (2006) Estimating saturated hydraulic conductivity in spatially variable fields using neural network ensembles. *Soil Sci Soc Am J* 70:1851–1859
- Pierzynski GM (2000) *Methods of phosphorus analysis for soils, sediments, residuals and waters*. Southern Coop, Series Bull, No 396. North Carolina State Univ, Raleigh, NC, 102 pp
- Reading LP, Baumgart T, Bristow KL, Lockington DA (2012) Hydraulic conductivity increases in a sodic clay soil in response to gypsum applications: impacts of bulk density and cation exchange. *Soil Sci* 177:165–171
- Reynolds WD, Elrick DE (1986) A method for simultaneous in situ measurement in the vadose zone of field-saturated hydraulic conductivity sorptivity and the conductivity-pressure head relationship. *Ground Water Monit Rev* 6:84–95
- Riitters KH, O'Neill RV, Hunsaker CT, Wickham JD, Yankee DH, Timmons SP, Jones KB, Jackson BL (1995) A factor analysis of landscape pattern and structure metrics. *Landscape Ecol* 10:23–39
- Romano N, Palladino M (2002) Prediction of soil water retention using soil physical data and terrain attributes. *J Hydrol* 265:56–75
- US Salinity Laboratory Staff (1954) *Diagnosis and improvement of saline and alkali soils*. US Dept Agriculture Handbook 60, US Government Printing Office, Washington DC, 160 pp
- Salter PJ, Williams JB (1965) The influence of texture on the moisture characteristics of soils II Available water capacity and moisture release characteristics. *J Soil Sci* 16:310–317
- Schaap MG, Leij FJ (1998) Using neural networks to predict soil water retention and soil hydraulic conductivity. *Soil Till Res* 47:37–42
- Schaap MG, Leij FJ, van Genuchten MTh (1999) A bootstrap-neural network approach to predict soil hydraulic parameters. In: van Genuchten MTh, Leij FJ, Wu L (eds) *Proc. Int. Workshop, Characterization and Measurements of the Hydraulic Properties of Unsaturated Porous Media*, University of California, Riverside, CA, pp 1237–1250
- Schaap MG, Leij FJ, van Genuchten MT (2001) ROSETTA: a computer program for estimating soil hydraulic parameters with hierarchical pedotransfer functions. *J Hydrol* 251:163–176
- Schoeneberger PJ, Wysocki DA, Benham EC, Broderson WD (2002) *Field book for describing and sampling soils.*, version 2.0. Natural Resources Conservation Service, United States Department of Agriculture, National Soil Survey Center, Lincoln, Nebraska
- Shahi HN (1968) Soil moisture determination by saturation capacity approach. *Plant and Soil* 29:333–334
- Sharma V, Negi SC, Rudra RP, Yang J (2003) Neural networks for predicting nitrate-nitrogen in drainage water. *Agr Water Manag* 63: 169–183
- Shein EV, Arkhangel'skaya TA (2006) Pedotransfer functions: state of the art problems and outlooks. *Eurasian Soil Sci* 39:1089–1099
- Simunek J, Sejna M, van Genuchten MT (1998) *Code for simulating the one-dimensional movement of water heat and multiple solutes in variably saturated media*, version 2.01. US Salinity Laboratory, US Department of Agriculture, Riverside, California
- Sobieraj JA, Elsenbeer H, Cameron G (2004) Scale dependency in spatial patterns of saturated hydraulic conductivity. *CATENA* 55:49–77
- Soil Survey Staff (2010) *Keys to soil taxonomy*. United States Department of Agriculture, Natural Resources Conservation Service
- Stumpp C, Engelhardt S, Hofmann M, Huwe B (2009) Evaluation of pedotransfer functions for estimating soil hydraulic properties of prevalent soils in a catchment of the Bavarian Alps. *Eur J For Res* 128:609–620
- Tietje O, Hennings V (1996) Accuracy of the saturated hydraulic conductivity prediction by pedo-transfer functions compared to the variability within FAO textural classes. *Geoderma* 69:71–84
- Tietje O, Tapkenhinrichs M (1993) Evaluation of pedo-transfer functions. *Soil Sci Soc Am J* 57:1088–1095
- Tyler SW, Wheatcraft SW (1989) Application of fractal mathematics to soil water retention estimation. *Soil Sci Soc Am J* 53:987–996
- van Genuchten MTh, Leij FJ, Yates SR (1991) The RETC code for quantifying the hydraulic functions of unsaturated soils. EPA /600/ 2-91/065, US Environmental Protection Agency, Ada, OK
- Wagner B, Tarnawski VR, Hennings V, Müller U, Wessolek G, Plagge R (2001) Evaluation of pedo-transfer functions for unsaturated soil hydraulic conductivity using an independent data set. *Geoderma* 102:275–297
- Wagner B, Tarnawski VR, Stöckl M (2004) Evaluation of pedotransfer functions predicting hydraulic properties of soils and deeper sediments. *J Plant Nutr Soil Sci* 167:236–245
- Wang JR, Schmutge TJ (1980) *IEEE Trans Geosci Remote Sens* 18:288
- Wang Z, Chang AC, Wu L, Crowley D (2003) Assessing the soil quality of long-term reclaimed wastewater-irrigated cropland. *Geoderma* 114:261–278
- Wang XY, Chen XM, Li XL (2011) Saturated hydraulic conductivity of coastal soil with different degrees of salinization Jiangsu. *Agr Sci* 39:446–448
- Webster R, Oliver MA (1990) *Statistical methods in soil and land resource survey*. Oxford University Press, Oxford
- Wösten JHM, Pachepsky YA, Rawls WJ (2001) Pedotransfer functions: bridging the gap between available basic soil data and missing soil hydraulic characteristics. *J Hydro* 251:123–150
- Xu SH, Liu JL (2003) Advances in approaches for determining unsaturated soil hydraulic properties. *Advan Water Sci* 14:494–501
- Yao RJ, Yang JS, Chen XB, Yu SP, Li XM (2009) Fuzzy synthetic evaluation of soil quality in coastal reclamation region of north Jiangsu Province. *Sci Agric Sin* 42:2019–2027
- Yao RJ, Yang JS, Zhao XF, Chen XB, Han JJ, Li XM, Liu MX, Shao HB (2012) A new soil sampling design in coastal saline region using EM38 and VQT method. *Clean Soil Air Water* 40:972–979

- Yasin M, Muhammed S, Mian SM (1989) Hydraulic conductivity and ESP of soil as affected by sodic water. *Pakistan J Agric Res* 10:289–294
- Yu C, Loureiro C, Cheng JJ, Jones LG, Wang YY, Chia YP, Faillace E (1993) Data collection handbook to support modeling impacts of radioactive material in soil. Environmental Assessment and Information Sciences Division, Argonne National Laboratory, Argonne, IL
- Zhang JH, Liu JL, Zhang JB, Zhu AN (2010) Indirect methods to estimate saturated soil hydraulic conductivity in paddy soil of Changshu. *Chin J Soil Sci* 41:778–782